# Accurate Orientation-Free Indoor Positioning with Deep Convolutional Neural Network

Wenhua Shao*, Haiyong Luo†, Fang Zhao*, Cong Wang*, Antonino Crivello‡, Muhammad Zahid Tunio*
* School of Software Engineering, Beijing University of Posts and Telecommunications, Beijing, China
†Beijing Key Laboratory of Mobile Computing and Pervasive Device
†Institute of Computing Technology, Chinese Academy of Sciences, Beijing, China
‡Institute of Information Science and Technologies, CNR, Italy
‡University of Siena - Department of Information Engineering and Mathematics, Italy
E-mails: {shaowenhua, yhluo}@ict.ac.cn, {zfsse, wangc, zahid.tunio}@bupt.edu.cn, antonino.crivello@isti.cnr.it

***Abstract*—The smartphone-based indoor positioning has attracted considerable attentions over the past years. In order to implement accurate and infrastructure-free positioning systems, researchers have tried to fuse magnetic field, Wi-Fi and dead reckoning information applying particle filter technique. In fact, magnetic signals have high-resolutions and Wi-Fi signals are able to provide coarse-grained global results. However, in order to move particles, the particle filter requires the phone's orientation aligning with the user moving directions, thus limiting its applications and impairing user experiences. In order to implement an orientation-free, infrastructure-free and high precision positioning, we propose a deep learning based positioning scheme. The proposed scheme constructs a new kind of rich-information positioning image, then leverages the pattern study ability of convolution neural networks to automatically map positioning images to position-classification points. In order to generate enough positioning images for training the neural networks, we also present a position-classification points extracting and labeling method. Finally, experiments convincingly reveal that the proposed positioning network is orientation-free and achieves decent precisions.**

***Keywords—indoor positioning, orientation free, positioning images, convolutional neural networks***

## I. INTRODUCTION

Because of the growth of location-based services (LBS), indoor positioning has become a hot topic in the last years. Outdoor positioning system mainly builds on global navigation satellite system (GNSS). However, these satellite signals are attenuated by walls, thus becoming too weak for indoor positioning.

Researchers have developed various indoor positioning techniques to satisfy indoor LBS requirements. They utilize position signals including ultra wide band (UWB), radio frequency identification (RFID), echo, Wi-Fi, and magnetic field. UWB and RFID based schemes are high in positioning accuracy, but they need to deploy infrastructures [1,2]. Echo schemes are high in accuracy too, but dense sampling prevents it from continuous positioning in large scale [3]. Wi-Fi almost exists in every modern building, but Wi-Fi schemes are difficult to achieve high accuracy due to the fluctuation of signals, especially for moving pedestrians [4-8]. Researchers also tried to use the channel state information (CSI) [9,10] of Wi-Fi to implement high precision positioning, but the method need to sample a large number of dense training points, thus making it difficult to be implemented in large-scale applications. The indoor magnetic field is also ubiquitous due to the pervasive of the geomagnetic field, but magnetic schemes only achieve high precision in local areas [11-14].

Bahl and Padmanabhan first present RADAR [6], various Wi-Fi based indoor positioning system appears to further improve positioning accuracy and robustness [5,27,28]. The indoor magnetic field is stable and distinguishable in the local area, so researchers study its positioning features [15,17] and develop indoor positioning systems using dynamic time warping and probability model [11,16].

Wi-Fi and magnetic field signals are pervasive and complementary, so researchers have tried to combine them to implement an accurate and global-available indoor positioning scheme. Shu et al. [12] combine the RADAR [6] and the magnetic positioning with particle filter, achieving good accuracy. However, this method needs to restrict smartphone orientation aligning with the user moving direction, which is not often detectable. Another drawback is the scheme need to sample Wi-Fi and magnetic training data separately because of their different positioning principles, which increases sampling and environment survey workloads.

To solve these problems, we present a fusion positioning scheme powered by the emerging deep learning techniques. The proposed scheme utilizes Wi-Fi and magnetic field as positioning signals because of their ubiquity and complementary features. Deep Convolutional Neural Network (CNN) has a strong ability to automatically learn patterns from training data, which is suitable for indoor positioning.

Deep learning is the fastest-growing field in machine learning with the development of massive amounts of computational power. With deep learning, researchers have used surveillance camera to localize vehicles, and channel state information (CSI) to localize laptops [9,29]. A group fuses cameras and magnetic field with the neural network, but this method restricts phone's orientation to be upright to use the camera [30]. Researchers also try to implement indoor positioning Wi-Fi fingerprint based using backpropagation neural networks. However, these methods need massive fingerprint sampling work [31]. To the best of our knowledge, there is no other approach for fusion indoor positioning with convolutional neural network.

The contributions of the paper are three fold.

i. The paper introduces a magnetic/Wi-Fi positioning-image-expressing scheme to convert positioning signals into positioning images, enabling more methods to improve positioning performances.

ii. We design a positioning CNN with the support of the positioning images. The new model leverages a directed acyclic graphs (DAG) structure to eliminate the feature differences of Wi-Fi and magnetic signals, and implements orientation-free, infrastructure-free and high-precision positioning.

iii. The paper presents a positioning features identification and labeling method for position-classification points to generate mass training data sets for the positioning CNN.

The structure for the rest of this paper is as follows. Section II provides a background of Wi-Fi/magnetic signals and introduces the structure of the positioning image. Section III gives an overview of the positioning system, presents the fingerprint clustering and labeling method, and details the positioning CNN approach. Section IV conducts extensive experiments to evaluate the proposed positioning scheme. Finally, Section V concludes the whole paper describing conclusion and future works.

## II. Features Description and Positioning Images

The proposed positioning algorithm leverages magnetic fields and Wi-Fi signals as location features. This section introduces the attributes of the features extracted from the two signals. Successively, the structures of positioning images are presented and explained.

### *A. The Attributes of Positioning Signals*

Magnetic fields and Wi-Fi are two important indoor positioning signals for smartphone based applications, because they are easy to be detected and are infrastructure-free. The two signals are complementary in the way that they provide location information.

Indoor magnetic fields have decent discernibility in local areas, and are able to keep static for a long term, but their discernibility decreases as comparing area enlarges [15-17]. For example, Fig. 1 illustrates two magnetic fingerprints gathered along a corridor in the March and May. The similarity of the two fingerprints reflects the stability of magnetic field. For the local discernibility example, let us assume that a user measures a magnetic strength of 50 $\mu T$. If we have a priori knowledge that the user's rough position is around the 40~55 meters, we can refine positioning results by comparing magnetic strengths, and estimates that the user is at the 50 meters position with an error less than one meter. However, without this local area prerequisite, we have to average all eligible positions with magnetic strength of 50 $\mu T$, leading to decreased accuracies.

The uniqueness of Wi-Fi media access control (MAC) address and its limited signal coverage range enable it for global positioning. However, it is difficult to for Wi-Fi to implement high-accuracy positioning for moving smartphones.

First, Wi-Fi signals are susceptible to surrounding electromagnetic noises like transmission rate and power adaptions [18], causing signal strengths fluctuates with time, thus confusing with nearby positions.

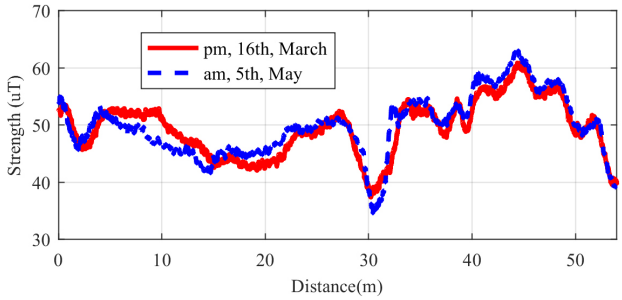


Fig. 1 Stability of indoor magnetic field strength. The two fingerprint traces have been gathered along a 52 meters corridor with an interval of two months.

Second, the signal scanning process takes several seconds to traverse all channels, therefore, users have left several meters from the sampling point when the scanning process finished, especially for those statistic-based methods [5,19] that need several scanning period to collect enough samples in one place to fit signal distributions.

### *B. The Structure of a Fingerprint Image*

Different from the traditional feature extraction manners of position signals, we propose a novel image method. In a narrow sense, a color image is a three-dimensional matrix, defined by width, height and color channels (red, green, and blue). Similarly, we define positioning fingerprint images as a two-dimensional matrix. Sensor data sequences are one-dimensional time series containing multiple feature channels. In order to save sensor data as images, we use the first dimension of fingerprint images to represent the length of the sensor sequence, and the second dimension to represent feature channels, in other words, image width and height respectively.

CNNs demand the size of all input images must be the same, so we need to normalize these fingerprint images into a standard size, as shown in Fig. 2. The normalized image width $n$ is defined by the fingerprint length r and storage density $\rho$:

$$n = 2 \cdot round(r \cdot \rho) + 1 \tag{1}$$

where the balanced structure guarantees the classification point laying in the center of the fingerprint image. The fingerprint image $F^{wm}$ can be represented as:

$$\begin{cases} F^{wm} = \begin{bmatrix} F^m \\ F^w \end{bmatrix} \\ F^m = [MS_1, MS_2, \cdots, MS_n] \\ F^w = \begin{bmatrix} RSSI_{11} & RSSI_{12} & \cdots & RSSI_{1n} \\ RSSI_{21} & RSSI_{22} & \cdots & RSSI_{2n} \\ \cdots & \cdots & \cdots & \cdots \\ RSSI_{m1} & RSSI_{m2} & \cdots & RSSI_{mn} \end{bmatrix} \end{cases} \tag{2}$$

where $F^m$ is the magnetic fingerprint image part, and $F^w$ is the Wi-Fi part. $F^{wm}$ is resampled to fit the image with $n$.

The height normalizations of fingerprint images are different for the magnetic and Wi-Fi parts. Magnetic parts only adopt strengths as magnetic field features, so the magnetic strengths $F^m$ are stored as a $1 \times n$ vector. The Wi-Fi part is stored as a $m \times n$ matrix, where the height $m$ is equal to the number of all

Wi-Fi MAC addresses detected in the positioning area, in detail, equaling to the number of the different mac addresses. Elements in Wi-Fi parts are received signals strength indexes (RSSIs) gathered from access points. In order to keep the consistency of fingerprint images, the RSSI of an access point (AP) at point $P_x$ whose strength cannot be detected is set to -120dB.

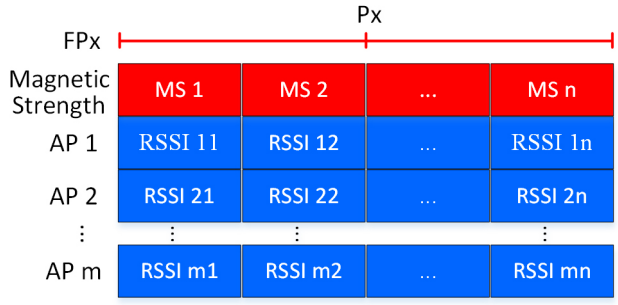


Fig. 2 Fingerprint image. Here, Px is a classification point. MS means magnetic strength. RSSI stands for received signal strength index. FPx is the fingerprint at classification point Px. The width of this fingerprint image is n, the height is m+1.

## III. The Proposed Solution

In order to explain the positioning solution proposed in this work, we introduce in part A the system's architecture. Part B is focused on acquiring training data. Finally, in part C, we propose the CNN based positioning method.

### A. System Architecture

As Fig. 3 shows, the proposed system consists of five modules: fingerprint clustering, network training, step detector, fingerprint normalization, and CNN positioning. In addition, a sensor module in smartphones provides the metadata of Wi-Fi, magnetic and acceleration signals to upper modules continuously. The working process can be divided into two phases:

1) *Training phase:* First, we uniformly generate position points within reachable areas, then the system clusters and labels position fingerprints with the nearest position point. Finally, we train a positioning neural network with the labeled fingerprints. The detailing clustering and labeling method is discussed later.

2) *Positioning phase:* First, the step detector detects step events and estimates user moving distances with a frequency module [20]. The step events are used to intrigue positioning estimations, and the moving distances are used to measure fingerprint lengths. Then, real-time fingerprints are resampled by the normalization module with the assigned density and length to conform the standard of CNN module. Finally, the CNN module estimates user locations by comparing real-time fingerprints against positioning neural networks.

### B. Fingerprint Clustering and Labeling

The proposed system leverages classification methods to localize real-time positioning fingerprints. Therefore, the system discretizes continuous indoor positions into separate classification points. In order to achieve high positioning accuracy, the classification points should be dense enough. In training phase, features near these classification points are needed to be sampled to train positioning neural networks. In our practice, a tester inputs the nodes of a sample line, and then he holds a smartphone, and walks along the line at a uniform speed (~1 m/s).

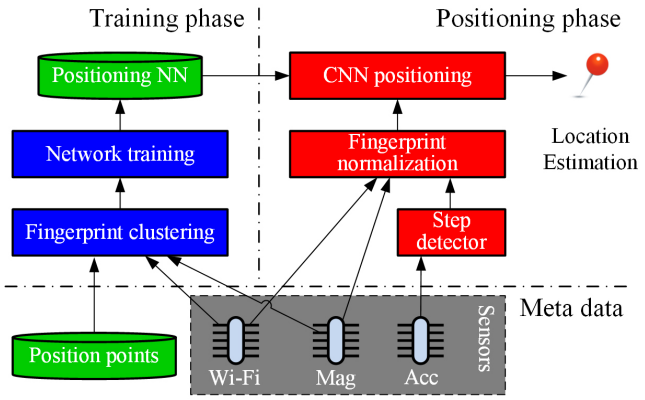


Fig. 3 The overall system architecture. Here, Acc means a triaxial accelerometer. Mag means a triaxial magnetometer. Wi-Fi is the Wi-Fi communication chip. NN means neural networks. CNN means convolutional neural networks.

As Fig. 4 shows, sample lines could be straight like the fingerprint one, or polygonal like fingerprint two that samples an intersection. Then fingerprint segments lie within the detection circle of classification point P are extracted as potential features of point P. Successively, the lengths of potential feature segments and the diameter (2r) of the detection circle are compared. The approximate segments are labeled with point P.

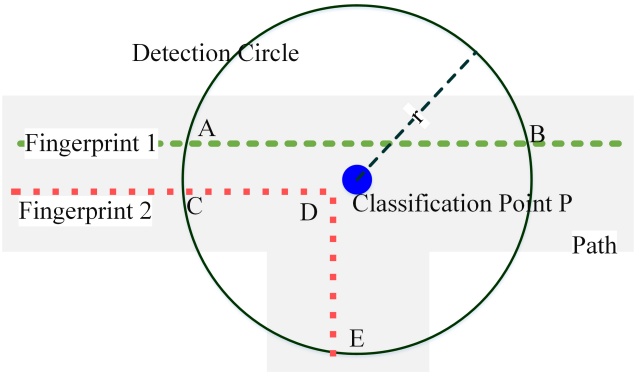


Fig. 4 Fingerprint clustering and labeling. Fingerprints into the detection circle are labeled belonging to point P. As light gray is shown a T shape corridor.

In order to accelerate network training, fingerprint images are normalized at last. Research shows that CNN convergence is usually faster if the average of each input variable over the training set is close to zero [21]. Therefore, the scheme calculates an average image from all the training images, then, normalizing both training and positioning images by subtracting the average image.

### C. Positioning CNN

Wi-Fi and magnetic fingerprint parts in the positioning image reveals different characters, so it is difficult to directly extract position patterns from the image with a single convolution window. In order to reduce the difference, we

propose that utilize two different convolution networks preprocess the position images first, then estimate the final location with another convolution network. As **Errore. L'origine riferimento non è stata trovata.** reveals, the proposed positioning neural network consists of three parts, forming a directed acyclic graph (DAG) structure.

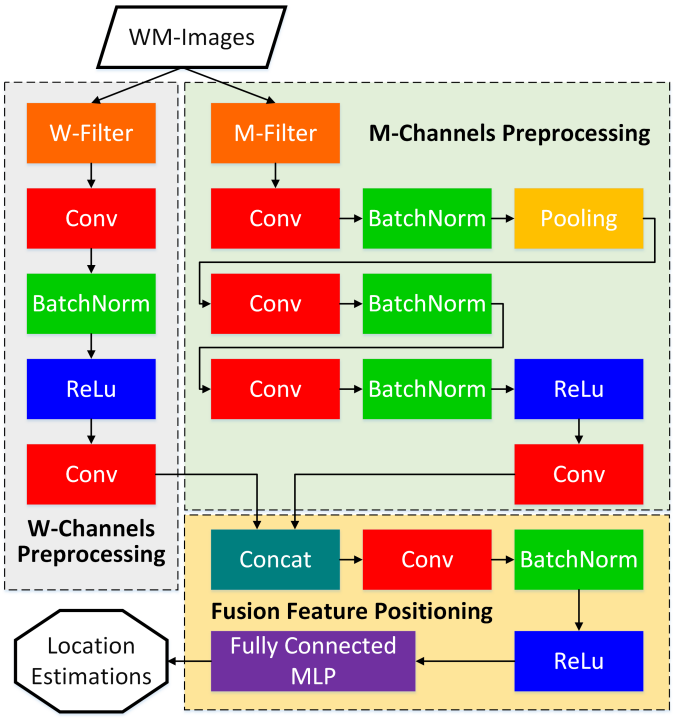


Fig. 5 Deep positioning neural network. The network consists of three branches: the Wi-Fi branch, the magnetic branch, and the fusion feature branch. The concat module is the responsible module for concatenation. The proposed algorithm is built on top of MatConvNet [22], an open source development platform for neural networks.

The Wi-Fi preprocessing network first leverages a W-Filter to isolate magnetic image parts and only keeps Wi-Fi image parts. The network uses the first convolution layer to extract features from input images, followed by a batch norm layer to accelerate convergence, then, a ReLu layer to add nonlinearity, finally another convolution layer converts extracted features to predication indexes. The simple structure helps it reducing overfitting problem. In detail, the convolution layer slides a random initialized convolution window along the input fingerprint, generating a new feature map. In practice, this layer has $H_1$ convolution windows with length of $W_1$, so the layer will generate $H_1$ new feature maps. Suppose the stride length of the windows is $S_1$, then, elements on generated maps can be represented as:

$$\begin{cases} y_{i_2,k_2} = b_{k_2} + \sum_{i_1=1}^{W_1} \sum_{j_1=1}^{m} \omega_{i_1,j_1} \cdot F^f_{i_2 \cdot S_1 + i_1, j_1, k_2} \\ 1 \le i_2 \le 1 + \left\lfloor \frac{n - W_1}{S^1} \right\rfloor \\ 1 \le k_2 \le H_1 \\ F^f \in \{F^m, F^w\} \end{cases} \quad (5)$$

where $\omega_{i_1,j_1}$ is an element on the convolution windows. Symbol $F^f_{i_2+i_1,j_1,k_2}$ is an element on the fingerprint images. Symbol $b_{k_2}$ is the bias of a convolution window. The batch normalization layer normalizes the activations of the previous layer at each batch by applying a transformation that maintains the average activation close to zero and the activation standard deviation close to one, to accelerate network convergence [26]. The ReLu layer is a nonlinear activation function, which adds non-linearity to the network. It helps in accelerating network convergence and improve network performance [24,25]:

$$y_{i_5,k_5} = \max\{0, y_{i_4,k_4}\} \quad (7)$$

Similarly, the magnetic preprocessing network leverages a M-Filter to select magnetic image parts. It utilizes a deeper CNN to increase network freedoms. The High freedom increases network's ability to mining complex position features, which is suitable for the static magnetic fingerprint. The network consists of nine layers: three convolution layers for features mining, three batch normalization layers to accelerating training convergence, one max pooling layer to reduce data size, one rectified linear unit layer for adding nonlinearity, and the final convolution layer converts extracted features to predication indexes — the same type of data as Wi-Fi preprocessing outputs.

Besides, the pooling layer reduces the data size by down-sampling the feature maps generated by the previous layer, and still keeps the main features. The proposed system applies a max-pooling layer, it leverages a max filter to the sub-regions of the initial feature map and takes the max of that region, creating a new output matrix where each element is the max of a region in the original input:

$$\begin{cases} y_{i_4,k_4} = \max\limits_{1 \le i_3 \le W_3} y_{i_4 \cdot S_3 + i_3, k_4} \\ 1 \le i_4 \le 1 + \left\lfloor \frac{\max(i_2) - W_3}{S^3} \right\rfloor \\ 1 \le k_4 \le \max(k_2) \end{cases} \quad (6)$$

where $W_3$ and $S_3$ are the window with and stride of the max pooling filter.

Because the preprocessing networks of Wi-Fi and magnetic preprocessing has convert the two heterogeneous signals into the same kind of data — predication indexes. Therefore, the fusion feature positioning module concatenates the two predication indexes vectors to form an isomorphic feature image, and utilizes convolution window to extract features inside the concatenated feature image.

Finally, a fully connected MLP calculates prediction values of all labels. This layer is a special case of the convolutional layer when the convolutional window width $W_6 = \max(i_5)$. The number of convolutional windows $H_6$ equals to the number of ground truth labels $C$. Therefore, this layer generates a prediction vector $y_{i_6}$ $(i_6 = 1{:}H_6)$. Every element in this vector is a score of the predicted labels. The predicted label with the highest scores is the final prediction.

After the abovementioned positioning neural network design, we need to train the network from the scratch. First, weights of the networks are randomly initialized. Then training procedures inputs the network with position labels and their feature segments, and utilizes a loss function to adjust the

weights with a BP algorithm. The proposed positioning loss function adopts a soft-max loss function. That is, for each piece of training data, we assign the ground truth label $c$ with an ordinal number, then the loss function is calculated with:

$$\ell = -\log \frac{e^{y_c}}{\sum_{i_6=1}^{C} e^{y_{i_6}}} \quad (8)$$

where $y_c$ is the prediction score of the ground truth label. Character $C$ is the total number of all the ground truth labels.

## IV. System Evaluation

This section evaluates the proposed positioning CNN in a variety of conditions. It starts with a description of the experimental environments and instrument specifications. Successively, evaluations on key coefficients used in the positioning CNNs are shown. Finally, a further applicable tests with different devices, users, and scenarios are discussed.

### A. Experiment Setup

We tested our positioning model in a real scenario with two commercially available smartphones — a HTC OneX and a Huawei Mate8 — to collect indoor magnetic field and Wi-Fi fingerprints. The smartphones sent real-time data to a PC server on each step event. Then the server calculated positioning results. It took about 2 milliseconds for each request. Training data were collected by the OneX, and was used to train the positioning model. The performance of the trained CNN model was tested on real-time positioning data from both OneX and Mate8.

Experiments were conducted on the seventh floor of an office building. The test bed covers an area of $60m \times 40m$, with a ceiling of $3m$ high. The testbed consists of office rooms and open working areas with many workstations, as Fig. 6 reveals. The test bed are divided into two scenarios: corridors and open areas. Corridors are paths along rooms, so more accurate Wi-Fi and magnetic field features are expected comparing to data gathered in open working areas.

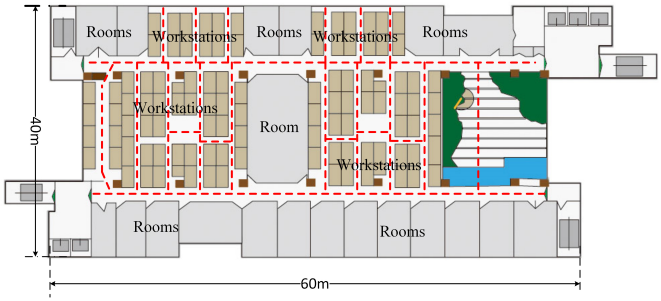


Fig. 6 The floor plan of the testing environment. The red dash lines are data collection paths. Gray blocks stand for office rooms. Orange blocks stand for workstations.

All the positioning accuracies are tested for moving pedestrian, with a testing length greater than 150 meters. Testers collect data of all sample lines for four times. There are 533 classification points inside the walking area.

### B. Positioning Performances at Different Device Orientations

In order to compare the model's performances with different smartphone headings, we ask a tester to hold a smartphone in four manners—forward portrait, backward portrait, leftward landscape, and rightward landscape, as Fig. 7 shows—then walking ahead. The forward portrait mode is the most common application scenario. In this mode, the e-compass orientation aligns with the user moving direction. In backward portrait mode, the e-compass orientation is inverse with the user moving direction. Landscape mode is common for games, like LBS augmented-reality games. In leftward and rightward landscape modes, e-compass orientations are vertical to the user moving directions. Positioning CNNs is trained with data collected in four orientations, one time for each.

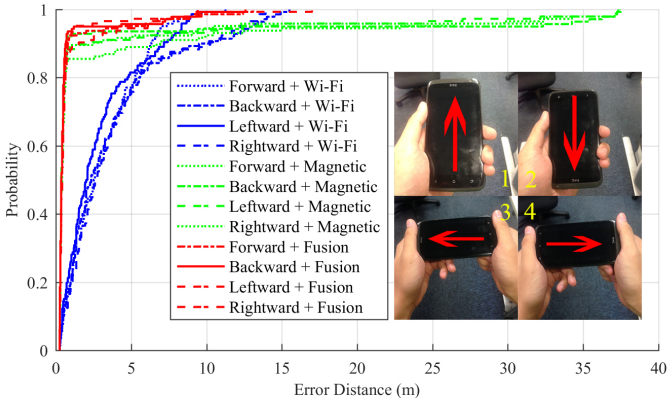


Fig. 7 Positioning performances of positioning CNNs with respect to different smartphone orientations. This experiment tests the smartphone in four orientations: 1, forward; 2, backward; 3, leftward; and 4, rightward.

As Fig. 7 shows, positioning accuracies are tested with different headings. In order to investigate the contributions of Wi-Fi and magnetic fingerprint parts, we also isolate Wi-Fi and magnetic fingerprint parts separately, and observe the performance of single fingerprint parts. The experiment results reveal that the positioning performances are approximate under different smartphone headings for Wi-Fi part, magnetic part and their combination fingerprint, because of sufficient trainings from all directions. It is worth noticing that the lowest accuracies of Wi-Fi are better than that of magnetic, and the highest accuracies of magnetic are better than Wi-Fi, in accordance with the previous signal analysis of Wi-Fi and magnetic. The fusion image performs better than both of single Wi-Fi and magnetic fingerprint, thus proving the proposed positioning model successfully exploits both advantages form the fusion positioning image.

### C. Positioning Performance of Different Users

This experiment tests the performances of the proposed scheme with different users. Because the proposed positioning CNN uses constant step lengths as estimated fingerprint image lengths. However, users have different stride lengths, so the step length estimation errors might affect the positioning performances. In the experiment, user #1 first collect training data to train the positioning CNN. Then nine users—two females and seven males, including the training user—walk inside the positioning area to test the positioning accuracies. The positioning accuracy of user #1 is better than other users, as Fig. 8 shows, because the CNN is trained with the data collected by the same person. In order to test the time stability of the proposed method, the training user test the CNN two week later.

The overall result is stable, but the low accuracy part becomes drops. This is because the lack of Wi-Fi training data, suggesting that we need more training data for Wi-Fi data. Therefore, in order to improve the model's generalization ability, the proposed CNN needs more users training data or data that is artificially generated from existing data.

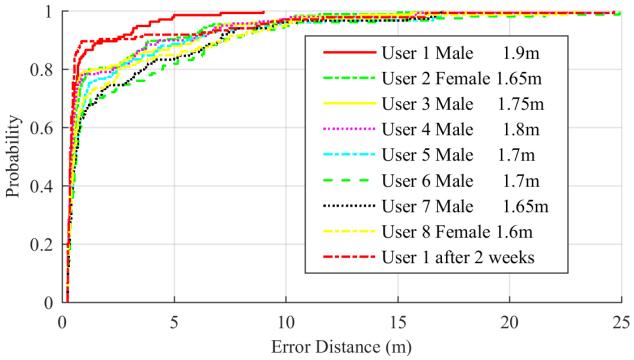


Fig. 8 Positioning performances considering different users.

### *D. Positioning Performance in Different Scenarios*

The proposed CNN is also tested in two different scenarios: corridors and open working areas. As Fig. 9 shows, the performances in corridors are better than that of open working areas. There are several reasons for the performance differences. In corridor scenarios, walls attenuate Wi-Fi signals, making them more distinguishable for different location points. But in open area scenarios, workstations in this area are only 1.5 meters high, so the Wi-Fi attenuation effect of work stations are much weak than that of walls. On the other hand, for magnetic signals, the workstations are mainly made of wood and aluminum materials, and the corridors consist of pillars and walls which containing lots of iron steels. Therefore, the magnetic distortion effect in open areas is not as good as that of corridors. Although the performance of open offices is weaker, it is acceptable for most indoor LBS applications.

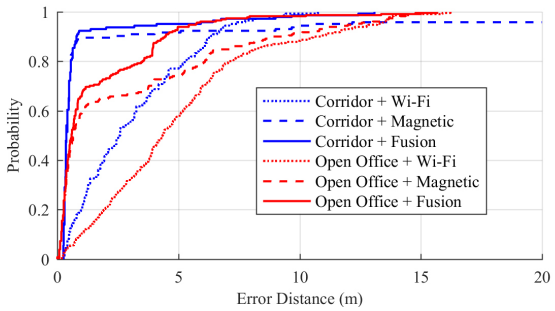


Fig. 9 Positioning performance in corridors and open working areas. We compare the changes of all three positioning CNNs.

## V. Conclusions and Future Work

We propose an accurate orientation-free indoor positioning system, utilizing RSSIs of existing Wi-Fi access points and strengths of the pervasive indoor magnetic field. Fusing this two kinds of position signals with deep learning is the basis of our scheme to achieve accurate positioning. Distinctive from previous fusion positioning method that design algorithms to fit positioning signals properties, our system leverages CNN to build up the mapping between location fixes and positioning signals automatically. Because of the fingerprints' insensitivity to smartphone orientations and CNN's feature-finding ability from multiple training data, the proposed positioning scheme achieves orientation-free function. In order to utilize deep learning technology inside indoor positioning field, we also design an indoor position labeling method and an image construction method for positioning fingerprints.

In order to train the positioning CNN, we need multiple-time samples to overcome overfitting problem. For future work, we plan to develop schemes to artificially expanding the training data from sparse samples to reduce sampling workload.

## Acknowledgment

This work was supported in part by the National Key Research and Development Program (2016YFB0502004), the National Natural Science Foundation of China (61374214), the BUPT Excellent Ph.D. Students Foundation (CX2017404), and the Open Project of the Beijing Key Laboratory of Mobile Computing and Pervasive Device.

## References

1. Zhang, G.; Rao, S.V. In *Position localization with impulse ultra wide band*, IEEE/ACES International Conference on Wireless Communications and Applied Computational Electromagnetics, 2005., 3-7 April 2005, 2005; pp 17-22.
2. Guo, Y.; Yang, L.; Li, B.; Liu, T.; Liu, Y. In *Rollcaller: User-friendly indoor navigation system using human-item spatial relation*, IEEE INFOCOM 2014 - IEEE Conference on Computer Communications, April 27 2014-May 2 2014, 2014; pp 2840-2848.
3. Liu, K.; Liu, X.; Xie, L.; Li, X. In *Towards accurate acoustic localization on a smartphone*, 2013 Proceedings IEEE INFOCOM, 14-19 April 2013, 2013; pp 495-499.
4. Wu, K.; Jiang, X.; Youwen, Y.; Min, G.; Ni, L.M. In *Fila: Fine-grained indoor localization*, 2012 Proceedings IEEE INFOCOM, 25-30 March 2012, 2012; pp 2210-2218.
5. Yang, S.; Dessai, P.; Verma, M.; Gerla, M. In *Freeloc: Calibration-free crowdsourced indoor localization*, 2013 Proceedings IEEE INFOCOM, 14-19 April 2013, 2013; pp 2481-2489.
6. Bahl, P.; Padmanabhan, V.N. In *Radar: An in-building rf-based user location and tracking system*, INFOCOM 2000. Nineteenth Annual Joint Conference of the IEEE Computer and Communications Societies. Proceedings. IEEE, 2000; Ieee: pp 775-784.
7. Hernandez, N.; Ocana, M.; Alonso, J.M.; Kim, E. Continuous space estimation: Increasing wifi-based indoor localization resolution without increasing the site-survey effort. *Sensors-Basel* **2017**, *17*, 23.
8. Zhao, F.; Luo, H.; Zhao, X.; Pang, Z.; Park, H. Hyfi: Hybrid floor identification based on wireless fingerprinting and barometric pressure. *IEEE Transactions on Industrial Informatics* **2017**, *13*, 330-341.
9. Wang, X.; Gao, L.; Mao, S.; Pandey, S. Csi-based fingerprinting for indoor localization: A deep learning approach. *Ieee T Veh Technol* **2017**, *66*, 763-776.
10. Wu, K.; Xiao, J.; Yi, Y.; Chen, D.; Luo, X.; Ni, L.M. Csi-based indoor localization. *Ieee Transactions on Parallel And Distributed Systems* **2013**, *24*, 1300-1309.
11. Subbu, K.P.; Gozick, B.; Dantu, R. Locateme: Magnetic-fields-based indoor localization using smartphones. *Acm T Intel Syst Tec* **2013**, *4*.
12. Shu, Y.; Bo, C.; Shen, G.; Zhao, C.; Li, L.; Zhao, F. Magicol: Indoor localization using pervasive magnetic field and opportunistic wifi sensing. *Ieee Journal on Selected Areas In Communications* **2015**, *33*, 1443-1457.
13. Xie, H.; Gu, T.; Tao, X.; Ye, H.; Lv, J. Maloc: A practical magnetic fingerprinting approach to indoor localization using smartphones. In *UBICOMP*, SEATTLE, WA, USA, 2014.
14. Luo, H.; Zhao, F.; Jiang, M.; Ma, H.; Zhang, Y. Constructing an indoor floor plan using crowdsourcing based on magnetic fingerprinting. *Sensors-Basel* **2017**, *17*, 2678.
15. Angermann, M.; Frassl, M.; Doniec, M.; Julian, B.J.; Robertson, P. Characterization of the indoor magnetic field for applications in localization and mapping. *2012 International Conference on Indoor Positioning And Indoor Navigation (Ipin)* **2012**.

16. Le Grand, E.; Thrun, S. *3-axis magnetic field mapping and fusion for indoor localization*. 2012; p 358-364.
17. Shao, W.; Zhao, F.; Wang, C.; Luo, H.; Muhammad Zahid, T.; Wang, Q.; Li, D. Location fingerprint extraction for magnetic field magnitude based indoor positioning. *J. Sens.* **2016**, *2016*, 16.
18. Wang, W.; Liu, A.X.; Shahzad, M.; Ling, K.; Lu, S. Understanding and modeling of wifi signal based human activity recognition. In *Proceedings of the 21st Annual International Conference on Mobile Computing and Networking*, ACM: Paris, France, 2015; pp 65-76.
19. Youssef, M.A.; Agrawala, A.; Shankar, A.U. In *Wlan location determination via clustering and probability distributions*, Proceedings of the First IEEE International Conference on Pervasive Computing and Communications, 2003. (PerCom 2003). 26-26 March 2003, 2003; pp 143-150.
20. Li, F.; Zhao, C.; Ding, G.; Gong, J.; Liu, C.; Zhao, F. A reliable and accurate indoor localization method using phone inertial sensors. In *Proceedings of the 2012 ACM Conference on Ubiquitous Computing*, ACM: Pittsburgh, Pennsylvania, 2012; pp 421-430.
21. LeCun, Y.A.; Bottou, L.; Orr, G.B.; Müller, K.-R. Efficient backprop. In *Neural networks: Tricks of the trade*, Springer Berlin Heidelberg: 2012; pp 9-48.
22. Gupta, A.V.K.L.A. Matconvnet convolutional neural networks for matlab.
23. LeCun, Y.; Boser, B.; Denker, J.S.; Henderson, D.; Howard, R.E.; Hubbard, W.; Jackel, L.D. Backpropagation applied to handwritten zip code recognition. *Neural computation* **1989**, *1*, 541-551.
24. Krizhevsky, A.; Sutskever, I.; Hinton, G.E. In *Imagenet classification with deep convolutional neural networks*, Advances in neural information processing systems, 2012; pp 1097-1105.
25. Maas, A.L.; Hannun, A.Y.; Ng, A.Y. In *Rectifier nonlinearities improve neural network acoustic models*, Proc. ICML, 2013.
26. Ioffe, S.; Szegedy, C. Batch normalization: Accelerating deep network training by reducing internal covariate shift. *arXiv preprint arXiv:1502.03167* **2015**.
27. Chi, Z.; Subbu, K.P.; Jun, L.; Jianxin, W. Groping: Geomagnetism and crowdsensing powered indoor navigation. *IEEE Transactions on Mobile Computing* **2015**, *14*, 387-400.
28. Retscher, G.; Tatschl, T. In *Indoor positioning using wi-fi lateration—comparison of two common range conversion models with two novel differential approaches*, Ubiquitous Positioning, Indoor Navigation and Location Based Services (UPINLBS), 2016 Fourth International Conference on, 2016; IEEE: pp 1-10.
29. Kumar, A.K.T.R.; Schäufele, B.; Becker, D.; Sawade, O.; Radusch, I. In *Indoor localization of vehicles using deep learning*, 2016 IEEE 17th International Symposium on A World of Wireless, Mobile and Multimedia Networks (WoWMoM), 21-24 June 2016, 2016; pp 1-6.
30. Liu, Z.; Zhang, L.; Liu, Q.; Yin, Y.; Cheng, L.; Zimmermann, R. Fusion of magnetic and visual sensors for indoor localization: Infrastructure-free and more effective. *Ieee T Multimedia* **2017**, *19*, 874-888.
31. Zhou, C.; Wieser, A. In *Application of backpropagation neural networks to both stages of fingerprinting based wips*, Ubiquitous Positioning, Indoor Navigation and Location Based Services (UPINLBS), 2016 Fourth International Conference on, 2016; IEEE: pp 207-217.